Full-Configuration-Interaction Study of the Metal-Insulator Transition in Model Systems: Li_N Linear Chains ($N = 2, 4, 6, 8$)

Valentina Vetere [a], Antonio Monari [b], Gian Luigi Bendazzoli [b], Stefano Evangelisti [a], and Beate Paulus [c]

[(a)] Université de Toulouse, CNRS, Laboratoire de Chimie et Physique Quantiques, 118, Route de Narbonne, F-31062 Toulouse Cedex - France

[(b)] Dipartimento di Chimica Fisica e Inorganica, Università di Bologna Viale Risorgimento 4, I-40136 Bologna - Italy

[(c)] Max Planck Institute for the Physics of Complex Systems Nöthnitzer Str. 38, D-01187 Dresden, Germany

* E-mail: stefano@irsamc1.ups-tlse.fr

September 26, 2007

Abstract

The Metal-Insulator transition is studied in a model systems with ab-initio methods. These are linear chains of equally spaced Lithium atoms. Different indicators of the Metal-Insulator transition (minimum of the energy gap, maximum of the localization tensor or of the polarizability) are used and discussed. It is shown that the different indicators give concordant results. FCI benchmark results involving a configuration space of more than 1 bilion determinants are also presented.

Keywords:

Metal-Insulator transition, Localization tensor, Electron polarizability, Full CI, Lithium chains

1 Introduction

The subject of metal-insulator (MI) transitions is well established in the scientific literature, and several types of MI transitions have been described. These transitions can be classified according to the interaction responsible of the insulating behaviour. For instance, according to F. Gebhard [1], in the so called Band, Peierls, and Anderson insulators the electron-ion interaction is dominating, while different types of transitions are due to the electron-electron interaction. In particular, a MI transition occurrs when the interatomic distance of a metallic system is sufficiently augmented, so that the electrons become localized on a given atom. This type of phase transition is called, in a broad sense, a *Mott transation*, after the pioneering work of N.F. Mott on this field (see reference [2]). Strictly speaking, it is possible to have a phase transition, and hence a MI transition, only in infinite systems. However, some of the elements that characterize a MI transition are alredy present even for sytems of moderate size. For this reason, in the following, the term "MI transition" will be used in a large sense also for finite systems. The advantage of dealing with finite systems (in particular, small systems) is that they can be accurately described by using sophisticated Quantum Mechanical methods. It is possible, in this way, to understand the phenomenon at a microscopic level.

In the past, the MI transition in a model system composed of ten Lithium atoms disposed on a ring had been studied by one of us by using Multi-Reference Configuration Interaction (MRCI) approaches [3]. In the present article, the behavior of linear Lithium chains with respect to a MI transition is investigated at Full Configuration Interaction (FCI) level. We notice that a FCI approach is particularly suited to describe a wave function having different characters. In fact, FCI permits to follow, in a continuous way, a changing-nature wave function, from the short-bond metallic to the long-bond insulating regions.

Four different Li_N chains have been considered in this work, containing an

even number of atoms going from two to eight: $N = 2, 4, 6, 8$. Odd values of n have been discarded, since they correspond to an open-shell ground state for the neutral system. For this reason, it is likely that even and odd chains go to the infinite limit by presenting different behaviour.

Linear chains, with respect to cyclic rings, have the clear drawback of showing border effects. They present, on the other hand, several computational advantages, particularly if the system is treated at a FCI level. Linear chains have a high $D_{\infty h}$ symmetry, (that is reduced to the abelian D_{2h} in actual FCI calculations), which considerably reduce the computational cost of a FCI calculation. Moreover, closed-shell ground states for the neutral rings follow the $n = 4m+2$ rule of aromatic systems, of which only the $n = 6$ case would be feasible with present-day FCI tecnology (with the chosen basis set). Finally, small rings have bond angles significantly different from linearity, so the comparison between different values of n can become problematic.

Several different criteria can be used to distinguish between the metallic and insulating phases, and it has been shown that these criteria are in fact equivalent [6]. They are:

1. Zero energy gap.

2. Infinite per-atom polarizability.

3. Infinite fluctuation of the position.

Of course, zero gaps and infinite fluctuations or polarizabilities can be found only in infinite systems. In a finite cluster, however, it is possible to find behaviors that clearly indicate a trend toward the infinite system.

The present article is organized as follows: In Section 2 the notion of MI transition is defined, and its main characteristics are discussed. Section 4 is about the tecnical details of the numerical computations presented in this article, while in Section 4 these computation results are presented and discussed.

Finally, Section 5 is devoted to conclustions and the discussion of further perspectives.

2 The Metal-Insulator Transition

The MI transition is characterized by a vanishing gap in the excitation spectrum of the extended system. In the case of a one-electron Hamiltonian, the excitation gap comes out to be the difference between the HOMO and LUMO energies. The situation for a two-electron Hamiltonian is more complex. The gap can be computed directly from the enegy differences when one electron is added to or subtracted from the system. As an alternative, one can use the one-electron energies defined in the formalism of the Extended Koopmans' Theorem (EKT), that can provide a generalization of the HOMO and LUMO energies.

Two other quantities play a central role in the description of the metal-insulator transition. These are the Electron Polarizability (per atom), $\alpha_{\beta\gamma}(\omega)$, and the Localization Tensor, $< r_\beta r_\gamma >_c$, which is defined as the cumulant of the second position momentum. It has been shown that these two quantities diverge in the case of a metallic system. Their definition and relevance with respect to the MI transition will be briefly illustrated in the following subsections.

It should be noticed that the polarizability is an *extensive* property, related to the behavior of the whole system. Since we compare finite systems having a different number of atoms, it is convenient to use *intensive* properties defined as the corresponding extensive quantities divided by the number of atoms, n. In the following, by polarizability we we will mean the *specific*, or *per atom* polarizability.

2.1 The Energy Gap

Let us consider a finite system having n electrons. For the sake of simplicity, we assume n to be even. The energy gap Δ is defined as the difference between the Ionization Potential (IP) and the Electron Affinity (EA) of the system:

$$\Delta \,=\, \mathrm{IP}{-}\mathrm{EA} \,=\, (E(n{-}1){-}E(n)){-}(E(n){-}E(n{+}1)) \,=\, E(n{+}1){+}E(n{-}1){-}2E(n) \tag{1}$$

In the case of a purely monoelectronic Hamiltonian, the ground-state total energy is given by the sum of the occupied-spinorbital energies,

$$E(n) \,=\, \sum_{i=1}^{n} \epsilon_i \tag{2}$$

On the other hand, the ionic ground states having $n-1$ and $n+1$ electrons have energies

$$E(n-1) \,=\, \sum_{i=1}^{n-1} \epsilon_i \,=\, E(n) - \epsilon_{\mathrm{HOMO}} \tag{3}$$

and

$$E(n+1) \,=\, \sum_{i=1}^{n+1} \epsilon_i \,=\, E(n) + \epsilon_{\mathrm{LUMO}} \tag{4}$$

respectively. Here ϵ_{HOMO} and ϵ_{LUMO} are the energies of the Highest Occupied Molecular Orbital (HOMO) and the Lowest Unoccupied Molecular Orbital (LUMO). The one-electron energy gap is given by

$$\Delta \,\equiv\, \epsilon_{\mathrm{LUMO}} - \epsilon_{\mathrm{HOMO}} \tag{5}$$

and it is often called the HOMO-LUMO gap.

The situation is different in the case of an Hamiltonian containing two-electron terms: in the case of a SCF wave function, it is still possible to define orbital energies (the eigenvalues of the Fock matrix), but the total energy now is not given by the sum of the orbital energies. However, if the $(n-1)$ and $(n+1)$ ionic wave functions are *approximated* by

$$|\Psi^{(n-1)}> = \, a_{\mathrm{HOMO}}|\Psi> \tag{6}$$

and

$$|\Psi^{(n+1)}> = a^{+}_{\mathrm{LUMO}}|\Psi> \tag{7}$$

respectively, the excitation gap Δ can be approximated by the HOMO-LUMO gap δ:

$$\Delta \;=\; E(n+1) + E(n-1) - 2E(n) \;\simeq\; \delta \;=\; \epsilon_{\mathrm{LUMO}} - \epsilon_{\mathrm{HOMO}} \tag{8}$$

This in nothing but the well known Koopmans' Theorem [**?**].

In many cases, the SCF approximation is not sufficient for an accurate description of the system, and the electron correlation must be taken into account via a post-SCF treatment. The energy gap can be defined as the difference between the IP and the EA of the system. As an alternative, generalized Koopmans' energies can be defined to the case of a many-determinat wave function. This is done in the formalism of the so called "Extended Koopmans' Theorem", as discussed in the following subsection.

2.2 The Extended Koopmans' Theorem

Let us consider an arbitrary wave function $|\Psi>$ in the Hilbert space of n electrons, $\mathcal{L}$, and let E be the corresponding energy, $E =< \Psi|\hat{H}|\Psi >$. In the EKT formalism, the Hamiltonian operator is diagonalized in the two Hilbert spaces $\mathcal{L}^{<} = \text{span}\{a_i|\Psi >\}$ and $\mathcal{L}^{>} = \text{span}\{a_i^{+}|\Psi >\}$. This is equivalent to diagonalize the Hamiltonian matrices $\mathbf{H}^{<}$ and $\mathbf{H}^{>}$ in presence of the metrics (overlap) $\mathbf{S}^{<}$ and $\mathbf{S}^{>}$, respectively. The matrix elements of the Hamiltonian matrices are given by

$$H_{ij}^{<} =< \Psi|a_i^{+}\hat{H}a_j|\Psi > \tag{9}$$

and

$$H_{ij}^{>} =< \Psi|a_i\hat{H}a_j^{+}|\Psi > \tag{10}$$

while the elements of the overlaps are

$$S_{ij}^{<} =< \Psi|a_i^{+}a_j|\Psi > \tag{11}$$

and

$$S_{ij}^{>} =< \Psi|a_ia_j^{+}|\Psi > \tag{12}$$

Two sets of generalized eigenvalues are obtained, $E_i^{<}$ and $E_i^{<}$, each one of them having in principle the same dimension of the orbital basis set (we assume in this discussion that n is even and $|\Psi >$ has spin projection S_z equal to zero). Because of the Variational Theorem, the eigenvalues $E_i^{<}$ and $E_i^{>}$ are upper bounds to the energies of the i-th state of the systems having $n-1$ end $n+1$ electrons, respectively.

It is customary to subtract from $E_i^{<}$ and $E_i^{<}$ the energy of $|\Psi >$, obtaining upper bounds to the ionization potentials and the electron affinities:

$$\epsilon_i^{<} = E_i^{<} - E \tag{13}$$

and

$$\epsilon_i^{>} = E_i^{>} - E \tag{14}$$

If the wave function $|\Psi>$ is the HF determinant, the energies $\epsilon_i^<$ are the energies of the occupied orbitals, while $\epsilon_j^>$ are the energies of the virtual ones. If, on the other hand, $|\Psi>$ is a correlated wave function, the one-electron energies $\epsilon_i^<$ and $\epsilon_j^>$ are the generalization of these quantities in the presence of electron correlation. In particular, $\epsilon^<$, defined as the highest energy among the $\epsilon_i^<$'s, corresponds to the HOMO energy, while $\epsilon^>$, which is the lowest one among the $\epsilon_j^>$'s, corresponds to the LUMO energy.

The Extended Koopmans' Theorem says that, if $|\Psi>$ is the *exact* wave function (which implies that we are in the limit of a complete basis set), the HOMO and LUMO energies are the exact IP and (up to a -1 factor) EA of the system. There has been a considerable amount of debate on the status of this "Theorem", and we do not want here to enter into this discussion. In this work, the upper-bound property of the EKT energies are used, in a *finite* basis set, to produce approximated energy gaps from correlated wave functions. Therefore, the Koopmans' energy gap will be given by the difference $\delta = \epsilon^> - \epsilon^<$.

2.3 The Localization Tensor

We indicate by $\hat{\mathbf{r}}$ the position operator of an electron. It is a vector operator, having cartesian components $\hat{r}_\beta$ (β=x, y, z). The operator $\hat{\mathbf{r}}_i$ will be the position operator associated to the i-th electron. The total position for the whole system is a one-electron operator, given by

$$\hat{\mathbf{R}} \;=\; \sum_{i=1}^{n} \mathbf{r}_i \tag{15}$$

It has three cartesian components $\hat{R}_\beta$ (β=x, y, z).

For any electronic wave function $|\Psi>$, one can compute the expectation value $<\mathbf{r}>=<\Psi|\hat{\mathbf{R}}|\Psi>$ having cartesian components $<r_\beta>=<\Psi|\hat{R}_\beta|\Psi>$. It is also possible to compute higher momenta associated to these operators with respect to the electronic wave function $|\Psi>$, and to perform a cumulant expansion of these momenta [6]. The cumulant of the quadratic fluctuation of the position is defined as

$$<r_\beta r_\gamma>_c = \frac{1}{n}\left(<\Psi|\hat{R}_\beta\hat{R}_\gamma|\Psi> - <\Psi|\hat{R}_\beta|\Psi><\Psi|\hat{R}_\gamma|\Psi>\right) \tag{16}$$

In the following, for the sake of simplicity of notation, the localization tensor $<r_\beta r_\gamma>_c$ will be simply indicated as $\rho_{\beta\gamma}$.

2.4 The Electron Polarizability

For the sake of simplicity, the case of the electronic ground-state wavefunction $|\Psi_0>$, with energy E_0, will be considered. The linear response of the system to an external oscillating electric field is determined by the complex polarizability tensor [11]. The usual electric polarizability is the real part of the complex tensor and it can be expressed in the spectral form:

$$\alpha_{\beta\gamma}(\omega) = \sum_{k>0} \left(\frac{<\Psi_0|r_\beta|\Psi_k><\Psi_k|r_\gamma|\Psi_0>}{E_k - E_0 - \omega} + \frac{<\Psi_0|r_\beta|\Psi_k><\Psi_k|r_\gamma|\Psi_0>}{E_k - E_0 + \omega} \right) \tag{17}$$

where $|\Psi_k>$ are the eigenvectors of the system, in ascending order of energy $k = 0, 1, 2, \ldots$.

From the computational point of view, it is more convenient to solve first the equations:

$$(H - E_0 \pm \omega)|\beta_\pm> = (r_\beta - <r_\beta>)|\Psi_0> \tag{18}$$

where $<r_\beta> = <\Psi_0|r_\beta|\Psi_0>$, and then compute the polarizability as a sum of the following scalar products:

$$\alpha_{\beta\gamma}(\omega) = <\beta_+|(r_\gamma - <r_\gamma>)|\Psi_0> + <\beta_-|(r_\gamma - <r_\gamma>)|\Psi_0> \tag{19}$$

The localization tensor can also be expressed in the spectral resolution form as:

$$<r_\beta r_\gamma>_c = <\Psi_0|r_\beta - <r_\beta>|(r_\gamma - <r_\gamma>)\Psi_0> = \sum_{k>\Psi_0} <\Psi_0|r_\beta|k><k|r_\gamma|\Psi_0> \tag{20}$$

In this way the similarities to the polarizability are emphasized: they are both properties of the state $|\Psi_0>$ of the system, although the other states enter into its definition via the sum over the excited stated. The localization tensor can be computed simply as the square norm of the r.h.s. of eq. (18).

By letting ω in eq. (17) be complex, $\Im\omega \to 0+$, and using the relation:

$$\frac{1}{x \pm i0} = P\frac{1}{x} \mp i\pi\delta(x) \tag{21}$$

(P denotes Cauchy's principal value), one has:

$$\begin{aligned} \Im\alpha_{\beta\gamma}(\omega) &= \pi \sum_{k>0} < \Psi_0|r_\beta|\Psi_k >< \Psi_k|r_\gamma|\Psi_0 > \\ &\times \quad [\delta(E_k - E_0 - \omega) - \delta(E_k - E_0 + \omega)] \end{aligned} \tag{22}$$

Therefore, one gets the following connection between the localization and the polarizability tensors:

$$< r_\beta r_\gamma >_c \quad = \quad \frac{1}{n\pi} \int_0^\infty \Im\alpha_{\beta\gamma}(\omega) d\omega \tag{23}$$

3 Computational Details

Four equally spaced chains, Li_2, Li_4, Li_6, Li_8, have been considered, with internuclear distances ranging from 3.0 to 12.0 bohr. The system symmetry is $D_{\infty h}$, although all the calculations were performed in the abelian subgroup D_{2h}. Due to the size of the FCI space (more than 10^9 symmetry-adapted Slater determinants in D_{2h}), only the internuclear values 4.0, 5.0, 6.0, 7.0, 8.0, 10.0, and 12.0 bohr have been considered for Li_8. For the same reason, large-distance polarizabilities (10.0 and 12.0 bohr) were not computed for this system. The SCF and FCI Koopmans gaps, δ_{SCF} and δ_{FCI}, were computed for all the systems from the wavefunction of the neutral systems Li_N. The exact gaps Δ, on the other hand, were computed from the FCI wavefunctions of the cations Li_N^+ and anions Li_N^-. Since the anion Li_8^- is too large to be treated at FCI level, only the Koopmans gaps δ were computed for Li_8.

Because of the size of the FCI space in the case of Li_8, our results can represent an useful benchmark to test the performance with respect to FCI of approximated (and more practical) methods. For this reason, we reported our FCI results, for the distances considered for Li_8 at the FCI level, in a series of tables. For completeness, the corresponding results obtained for the smaller chains were also reported. However, in order keep the size of this article not too large, most of these tables are reported as Supplementary Material, while our results are mainly presented in a graphical form.

We used the gaussian ANO basis set optimized by Widmark et al. [**?**]. In particular, the $3s1p$ contraction was selected for this work. This basis set is a very small one, consisting of only six Atomic Orbitals (AO) for each Lithium atom. For this reason, the present results must be considered essentially qualitative, expecially as far as second order properties (i.e., polarizabilities) are concerned. However, the reduced size of the basis set enabled us to perform FCI calculations up to the Li_8 chains, that would have been absolutely untreat-

able by using larger basis sets. The overall qualitatively behavior of the involved quantities is nonethless correctly reproduced even with this basis set.

The SCF calculations have been done by using the DALTON *ab initio* package [8], that was also used to produce the file containing the AO one- and two-electron integrals. The integrals were subsequently transformed on the Molecular Orbital (MO) basis set, via the Ferrara four-index transformation [9]. All the FCI calculations (total energy, Koopmans energies, localization tensor, polarizabilities, entropies) have been performed by using the Bologna FCI code [7], interfaced to the DALTON and the Ferrara transformation code via the Q5COST library [10]. In the FCI computation, the $1s$ electrons have been frozen at the SCF level. This makes a basis set of five MO's per Lithium atom for the FCI calculations.

From a computational point of view, the total energy, the Koopmans energie and the localization tensor are easily computed once the FCI wavefunction has been converged, and have therefore a similar computational cost. The computation of a component of the polarizability tensor, on the other hand, is performed analytically, via the solution of the linear system (18). Since its cost is comparable to the computation of the FCI eigenvector, only a selected subset of polarizabilites was computed for the Li_8 system.

4 Results and Discussion

In Table 1, the ground-state symmetry (in $D_{\infty h}$ symmetry) and the FCI-space size are reported for all the studied systems. The energy curves of the neutral systems are illustrated in Figure 1. In order to make the comparison between the different values of N, the energies *per atom* are plotted. There is a minimum between five and six bohr, whose depth and position do not depend strongly on the number of atoms. When N is incresed, the minimum tends to become deeper, and to be located at larger distances. For a comparison, the internuclear experimental distance is ??? for Li_2 and ??? for the bulk (metallic Lithium).

In Figures 2a the HOMO ($\epsilon^{<}_{\rm SCF}$) and the LUMO ($\epsilon^{>}_{\rm SCF}$) Koopmans energies are show for the SCF wavefunction. In Figure 2b, the corresponding energies for the FCI wavefunction, ($\epsilon^{<}_{\rm FCI}$ and $\epsilon^{>}_{\rm FCI}$) are reported. Notice that, in the distance range we have investigated, there are no changes in the symmetry of the frontier orbitals, either SCF or FCI. The HOMO and LUMO energies are smooth functions of the distance parameter R. The energy gaps, however, have a very different behavior at SCF and FCI level. This can be seen in Figure 3, where the SCF and FCI Koopmans gaps, $\delta_{\rm SCF}$ and $\delta_{\rm FCI}$, are reported. The SCF values show the behavior of a metallic system in the whole range of distances, with gaps that become smaller with increasing values of N and R. The FCI values show the same behavior at short distances. Indeed, for R values up to abour six bohr, the SCF and FCI gaps are numerically very similar. This is explained by the fact that the FCI wave function is strongly dominated by the SCF determinant at short distances. For large values of R, on the other hand, the FCI gap increases again, and tends to constant (i.e., to a value not depending on N). This corresponds to the HOMO-LUMO gap in the isolated atom.

In Figure 4, the exact gap $\Delta_{\rm FCI}$, computed from the $n-1$ and $n+1$ energies, are reported. From a comparison with Figure 3, it can be seen that the behavior

of δ_{FCI} and Δ_{FCI} is very similar, although the exact gaps are considerably smaller than the Koopmans' ones.

In Figure 5, the specific polarizabilities computed at the FCI level, are reported. The behavior of the perpendicular polarizability, $\alpha_{\perp}$, is shown in the Figure 5a. The values of $\alpha_{\perp}$ depend very weakly from N, with the tendance to a slight growth specific polarizabilities as the size of the system is increased. As a function of the interatomic distance, $\alpha_{\perp}$ increases as R increases, and tends monotonically to the constant value of an isolated lithium atom for large values of R. The specific parallel polarizabilities, $\alpha_{\parallel}$, on the other hand, have a completely different behavior (see Figure 5b, where the values of $\alpha_{\perp}$ are also reported for comparison). Short values of R show parallel polarizabilities numerically similar to the perpendicular ones. When R is increased, $\alpha_{\parallel}$ has a steep rising, up to a maximum located beween 6 and 7 bohr. The height of the maximum increases very quickly with increasing values of N. For even larger values of R, the polarizabilities decrease, down to the constant value of an isolated atom at large distances, with a behavior similar to $\alpha_{\perp}$.

The behavior of the localization tensor is shown in Figure 6, and is very similar to the trend shown by the polarizability. We plot the perpendicular and parallel components, $\rho_{\perp} =< r_x r_x >_c$ and $\rho_{\parallel} =< r_z r_z >_c$. It can be seen that the maximum of the parallel component grows slower than the polarizability as a function of N.

For an infinite system, the correlated energy gap (either δ or Δ) is zero for value of R that are shorter than the MIT distance. For larger distances, the gap grows until it reaches the isolated-atom value. Correspondingly, the (specific) parallel polarizability and parallel localization tensor show the opposite trand: they diverge before the MIT distance, then they lower to reach the isolated-atom values. For finite systems, and in absence of a MI transition, the excitation gap lowers as the distance parameter R increases (sse, for instance, the uncorrelated HOMO-LUMO gap of the SCF wavefunction). In a similar way, the specific

polarizability and localization tensor increse as a function of the R (see the perpendicular components).

In Table 2 the interpolated values (obtained via an exponential spline) are reported. Some important points should be remarked:

1. For a fixed length of the chain, the positions of the gap minimum and the polarizability maximum coincide remarkably.

2. The MIT distance shortens when the chain lenghth becomes longer, and it converges to a value close to 6.5 bohr.

Finally, it is a remarkable fact that the "signature" of the MI transition can already be see in the behaviour of the dimer.

5 Conclusions

From this investigation, it emerges that different possible indicators (energy gap, localization tensor, electron polarizability) present remarkably concordant behaviors with respect to the MI transition. In particular, the localization tensor and the electron polarizability have emerged as powerful tools to locate the transition between the metallic and insulating states. An important practical difference exists between these two indicators, as far as the computational cost is concerned: the localization tensor, can be straightforwardly computed from the wave function, the polarizability, on the other hand, is considerably more expensive, since it requires an additional iterative procedure whose cost is comparable with the eigenvector calculation.

Other important points that have emerged from the present study are the following:

1. For a fixed length of the chain, the positions of the gap minimum and the polarizability maximum coincide remarkably.

2. The MI Transition distance is not very sensitive to the chain length: it has a slight tendence to shorten for longer chains, converging to a value close to 6.5 bohr.

In the future, we also plan to study with the same approach other systems. A first aspect that will be considered, and that was already addressed in reference [3], is the emerging of a Peierls instability in these model systems. In particular, it will be interesting to compare the behavior of Lithium and Hydrogen model chains, both Peierls distorted and undistorted, with respect to the MI transition.

The investigation of beryllium linear chains, as well as three-dimensional clusters, will also be considered. Preliminary results indicate that the long-distance, insulating behavior of this closed-shell system can be correctly de-

scribed at Coupled-Cluster level. If this preliminary results are confirmed, this fact could open the way for the study of different and much larger systems.

Acknowledgements

This work was partly supported by the French (CNRS) and by the Italian Ministry of University and Research MUR and the University of Bologna for under the project "PRIN 2006. Molecular Quantum Mechanics: Computational Methods and Analysis of Novel Phenomena".

Figure Captions

- **Figure 1**: Energy per Li atom as a function of the nearest-neighbour distance parameter R (bohr). Distances in bohr and energies in hartree.
- **Figure 2**: HOMO and LUMO Koopmans' energies for the different wave functions as a function of the distance parameter R (bohr). **Figure 2a**: SCF wave function; **Figure 2b**: FCI wave function. Distance parameter R in bohr and energies in hartree.
- **Figure 3**: Koopmans' energy gaps as a function of the distance R. Distances in bohr and energies in hartree.
- **Figure 4**: Exact energy gaps as a function of the distance R. Distance in bohr and energy gaps in hartree.
- **Figure 5**: Specific (per atom) polarizabilities along the two main directions (orthogonal and parallel to the chain axes), as a function of the distance R. **Figure 5a**: $\alpha_\perp$; **Figure 5b**: $\alpha_\parallel$ ($\alpha_\perp$ is also reported for comparison). Distance in bohr and polarizabilities α in 10^3 bohr^3.
- **Figure 6**: Localization tensor along the two main directions ($\rho_\perp$ and $\rho_\parallel$, orthogonal and parallel to the chain axes, respectively), as a function of the distance R. Distance and localization tensor in bohr.

References

[1] F. Gebhard, "The Mott Metal-insulator Tansition: Models and Methods", Springer (1997).

[2] N. Mott, "Metal-insulator Transitions", 2nd edition, Taylor and Francis (1990).

[3] B. Paulus, K. Rosciszewski, P. Fulde, and H. Stoll Phys. Rev. B **68**, 235115 (2003).

[4] A.D. McLachlan and M.A. Ball, Rev. Mod. Phys. **36**, 844 (1964)

[5] W. Kohn, Phys. Rev. **133**, A171 (1964)

[6] R. Resta, J. Chem. Phys. **124**, 104104 (2006).

[7] Bendazzoli G. L., Evangelisti S., J. Chem. Phys., **98**, 3141-3150 (1993)

[8] DALTON, a molecular electronic structure program, Release 2.0 (2005) see http://www.kjemi.uio.no/software/dalton/dalton.html "

[9] R. Cimiraglia, C. Angeli private communication.

[10] Q5COST

[11] L.D. Landau, E.M. Lifshitz and L.P. Pitaevskij, Course of Theoretical Physics vol. 5, Statistical Physics part 1, Pergamon Press, Oxford New York Toronto Sydney Paris Frankfurt, 3rd Ed. 1980.

[12] P. Gori-Giorgi and P. Ziesche, Phys. Rev. B **66**, 235116 (2002)

Table 1: Li_N: Space and spin symmetry of the ground state and size of the symmetry-adapted FCI space (in the D_{2h} abelian group).

N	Li_N^+	Li_N	Li_N^-
2	$^2\Sigma_g$	$^1\Sigma_g$	$^2\Sigma_u$
	1	22	75
4	$^2\Sigma_u$	$^1\Sigma_g$	$^2\Sigma_g$
	660	5,524	29,748
6	$^2\Sigma_g$	$^1\Sigma_g$	$^2\Sigma_u$
	246,762	2,186,104	14,290,470
8	$^2\Sigma_u$	$^1\Sigma_g$	$^2\Sigma_g$
	not done	1,061,876,612	not done

Table 2: Li_N: SCF and FCI Total energies as a function of the internuclear distance. The isolated-atom corresponding values are (frozen core) E_{SCF}(Li) = E_{FCI}(Li) = -7.43262465. Distances are in bohr, energy gaps in hartree, and polarizabilities in 10^3 bohr^3.

SCF	d	$N = 2$	$N = 4$	$N = 6$	$N = 8$
	4.00	-14.85024547	-29.66571105	-44.48114926	-59.29661308
	5.00	-14.86985674	-29.72728195	-44.58479682	-59.44233333
	6.00	-14.86795025	-29.73163264	-44.59550369	-59.45939118
	7.00	-14.85829853	-29.71550118	-44.57287850	-59.43025981
	8.00	-14.84670478	-29.69351180	-44.54043316	-59.38734708
	10.00	-14.82541331	-29.65131653	-44.47723633	-59.30314149
	12.00	-14.80945254	-29.61917750	-44.42889039	-59.23859462
FCI					
	4.00	-14.87620066	-29.72907915	-44.58293809	-59.43769284
	5.00	-14.89355787	-29.78635638	-44.68124066	-59.57786284
	6.00	-14.89169861	-29.78994668	-44.69078071	-59.59365645
	7.00	-14.88406058	-29.77553528	-44.66903762	-59.56405701
	8.00	-14.87658813	-29.75874188	-44.64189291	-59.52562768
	10.00	-14.86831194	-29.73838454	-44.60853806	-59.47870722
	12.00	-14.86601182	-29.73254401	-44.59908516	-59.46561618

Table 3: Li_N^+ and Li_N^-: FCI total energies as a function of the internuclear distance. The isolated-atom corresponding values are $E_{FCI}(Li^+)$ = -7.23638894 and $E_{FCI}(Li^-)$ = -7.45039991. All values are in atomic units.

Li_n^+	d	$N = 2$	$N = 4$	$N = 6$
	4.00	-14.67278293	-29.55300414	-44.42206661
	5.00	-14.70282450	-29.62455313	-44.53512053
	6.00	-14.71018926	-29.63687571	-44.55276617
	7.00	-14.70799789	-29.62591325	-44.53327954
	8.00	-14.70218834	-29.60771794	-44.50287493
	10.00	-14.68919274	-29.57398543	-44.45027773
	12.00	-14.67957114	-29.55354289	-44.42258173
Li_n^-				
	4.00	-14.88132194	-29.76118256	-44.63259664
	5.00	-14.90492422	-29.83054348	-44.74445691
	6.00	-14.91052825	-29.84189051	-44.76063697
	7.00	-14.90911680	-29.83092649	-44.74058315
	8.00	-14.90544207	-29.81353523	-44.71048404
	10.00	-14.89773431	-29.78307551	-44.66018342
	12.00	-14.89207005	-29.76628940	-44.63562554

Table 4: HOMO Koopmans Enegies as a function of the internuclear distance. All values are in atomic units.

symmetry		σ_g	σ_u	σ_g	σ_u
$\epsilon^{<}_{\mathrm{SCF}}$	d	$N=2$	$N=4$	$N=6$	$N=8$
	4.00	-0.19231451	-0.17694282	-0.16893913	-0.16406892
	5.00	-0.18219323	-0.17053612	-0.16420830	-0.16035392
	6.00	-0.17229458	-0.16294062	-0.15776824	-0.15462125
	7.00	-0.16351713	-0.15592313	-0.15171986	-0.14919700
	8.00	-0.15603282	-0.14982364	-0.14644324	-0.14446988
	10.00	-0.14430437	-0.14015179	-0.13807050	-0.13696290
	12.00	-0.13556440	-0.13294895	-0.13178970	-0.13123707
$\epsilon^{<}_{\mathrm{FCI}}$					
	4.00	-0.20341773	-0.17672465	-0.16253815	-0.16406892
	5.00	-0.19073338	-0.16216117	-0.14773882	-0.13820065
	6.00	-0.18150936	-0.15363502	-0.13990398	-0.13092637
	7.00	-0.17606269	-0.15022760	-0.13843719	-0.14919700
	8.00	-0.17439979	-0.15160077	-0.14325885	-0.14446988
	10.00	-0.17911921	-0.16718413	-0.16500693	-0.13696290
	12.00	-0.18644068	-0.18222475	-0.18112430	

Table 5: LUMO Koopmans Energies as a function of the internuclear distance. All values are in atomic units.

symmetry		σ_u	σ_g	σ_u	σ_g
$\epsilon^{>}_{\mathrm{SCF}}$	d	$N=2$	$N=4$	$N=6$	$N=8$
	4.00	0.01855227	0.00525605	-0.00359676	-0.00999410
	5.00	0.01279972	-0.00816970	-0.02082225	-0.02885902
	6.00	0.00454250	-0.02003128	-0.03294678	-0.04061892
	7.00	-0.00430969	-0.02895103	-0.04074734	-0.04751403
	8.00	-0.01302943	-0.03543739	-0.04566980	-0.05142138
	10.00	-0.02875206	-0.04399802	-0.05088323	-0.05467068
	12.00	-0.04128767	-0.05003489	-0.05407774	-0.05627767
$\epsilon^{>}_{\mathrm{FCI}}$					
	4.00	0.01834771	0.00602595	-0.00134037	-0.00099941
	5.00	0.01357370	-0.00335100	-0.01263632	-0.01837059
	6.00	0.00796953	-0.00967050	-0.01836190	-0.02338542
	7.00	0.00389912	-0.01181192	-0.01895964	-0.04751403
	8.00	0.00273813	-0.00942851	-0.01447827	-0.05142138
	10.00	0.00878330	0.00429744	0.00332876	-0.05467068
	12.00	0.01722260	0.0156070	0.01550960	

Table 6: Energy gap as a function of the internuclear distance, computed by using different methods: K-SCF and K-FCI, Koopmans energies from the SCF and FCI wave functions, respectively; Δ-FCI, difference between IP and EA, both computed at FCI level. All values are in atomic units. **da finire!**

K-SCF	d	$N = 2$	$N = 4$	$N = 6$	$N = 8$
	4.00	0.21086677	0.18219887	0.16534236	0.15407482
	5.00	0.19499295	0.16236641	0.14338604	0.13149490
	6.00	0.17683709	0.12697210	0.12482146	0.11400233
	7.00	0.15920745	0.11438625	0.11097252	0.10168298
	8.00	0.14300338	0.12697210	0.10077344	0.09304849
	10.00	0.11555231	0.09615378	0.08718727	0.08229222
	12.00	0.09427673	0.08291406	0.07771196	0.07495940
K-FCI					
	4.00	0.22176544	0.18275060	0.16119778	0.15987860
	5.00	0.20430708	0.15881017	0.13510250	0.11983006
	6.00	0.18947889	0.14396452	0.12154208	0.10754095
	7.00	0.17996181	0.13841568	0.11947755	0.10735254
	8.00	0.17713792	0.14217226	0.12878058	0.12018504
	10.00	0.18790251	0.17148157	0.16833569	0.16086620
	12.00	0.20366328	0.19783175	0.19663390	
Δ-FCI					
	4.00	0.19829645	0.14397160	0.11121293	
	5.00	0.17936702	0.11761615	0.08290388	
	6.00	0.16267971	0.10112714	0.06815828	
	7.00	0.15100647	0.09423082	0.06421255	
	8.00	0.14554585	0.09623059	0.07042685	
	10.00	0.14969683	0.11970814	0.10661497	
	12.00	0.16038245	0.14525573	0.13996305	

Table 7: FCI polarizabilities as a function of the internuclear distance. The isolated-atom value is α(Li)=0.15877755. All values are in 10^3 atomic units. Distances are in bohr and polarizabilities in 10^3 bohr^3.

$\alpha_\perp$	d	$N=2$	$N=4$	$N=6$	$N=8$
	4.00	0.112384	0.177627	0.241159	
	5.00	0.132411	0.213600	0.291075	
	6.00	0.156679	0.256843	0.350309	
	7.00	0.185256	0.310080	0.426361	
	8.00	0.216084	0.372181	0.521581	
	10.00	0.265185	0.485127	0.703483	
	12.00	0.288586	0.546734	0.803787	
$\alpha_\parallel$					
	4.00	0.249337	0.995959	2.688216	
	5.00	0.351897	1.927794	6.943805	
	6.00	0.494519	3.141117	13.094996	
	7.00	0.624934	3.881995	15.522591	
	8.00	0.671242	3.499613	11.182665	
	10.00	0.531132	1.651295	3.093501	
	12.00	0.408018	0.974104	1.569960	

Table 8: FCI localization tensor as a function of the internuclear distance. The isolated-atom value is α(Li)=0.??????. All values are in bohr.

$r_\perp$	d	$N=2$	$N=4$	$N=6$	$N=8$
	4.00	6.78	11.97	17.04	
	5.00	7.50	13.45	19.23	25.10
	6.00	8.17	14.85	21.31	27.68
	7.00	8.81	16.26	23.50	31.68
	8.00	9.38	17.60	25.68	33.68
	10.00	10.15	19.52	28.85	38.17
	12.00	10.49	20.45	30.39	
$r_\parallel$					
	4.00	10.26	27.22	53.22	
	5.00	12.23	38.05	84.47	164.25
	6.00	14.64	49.47	117.55	266.32
	7.00	16.50	56.32	133.50	336.08
	8.00	16.93	54.18	117.27	216.96
	10.00	14.51	36.25	60.77	86.48
	12.00	12.48	27.27	42.41	

Table 9: The MI transition for the FCI wave function: minimum energy gap, $\delta_{\min}$, maximum longitudinal specific polarizability, $\alpha_{\max}$, and maximum position fluctuation, $r_{\max}$, with the corresponding interatomic distances, d_δ, d_α, and d_z, respectively. Distances are in bohr, energy gaps in hartree, and polarizabilities in 10^3 bohr^3

N	$\delta_{\min}$	$\delta - ex_{\min}$	$\alpha_{\max}$	$z_{\max}$	d_δ	$d_{\delta-ex}$	d_α	d_z
2	0.177	0.1453	335.79	16.97	7.92	8.26	7.93	7.76
4	0.138	0.0932	974.85	56.71	7.11	7.26	7.17	7.28
6	0.112	0.0641	2605.72	133.51	6.69	6.88	6.84	7.02
8	0.106			336.09	6.52			7.01

Figure 1: Energy per Li atom as a function of the nearest-neighbour distance parameter R (bohr). Distances in bohr and energies in hartree.

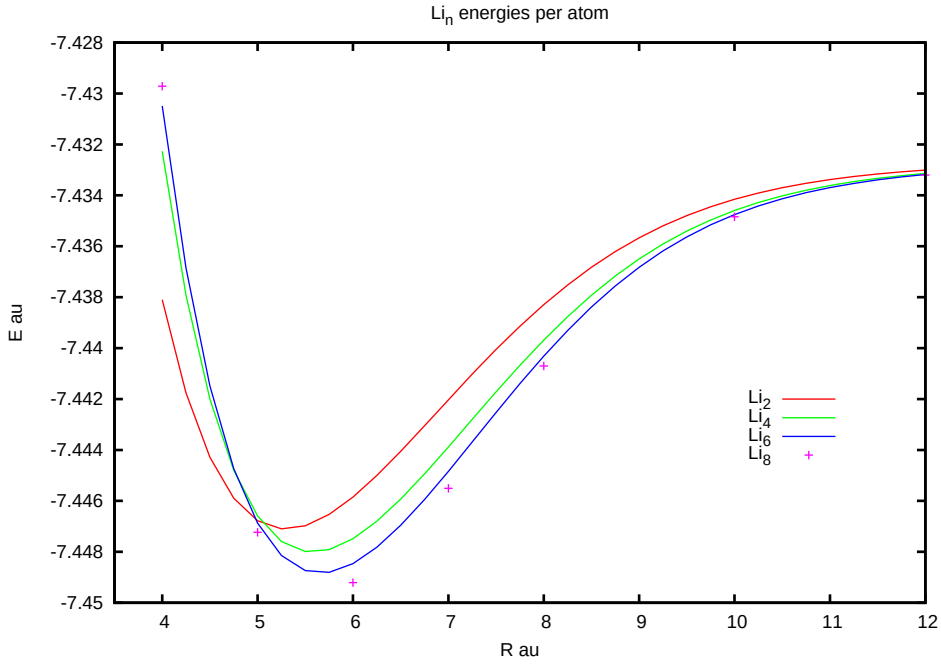

Figure 2: HOMO and LUMO Koopmans' energies for the different wave functions as a function of the distance parameter R (bohr). **Figure 2a**: SCF wave function; **Figure 2b**: FCI wave function. Distance parameter R in bohr and energies in hartree.

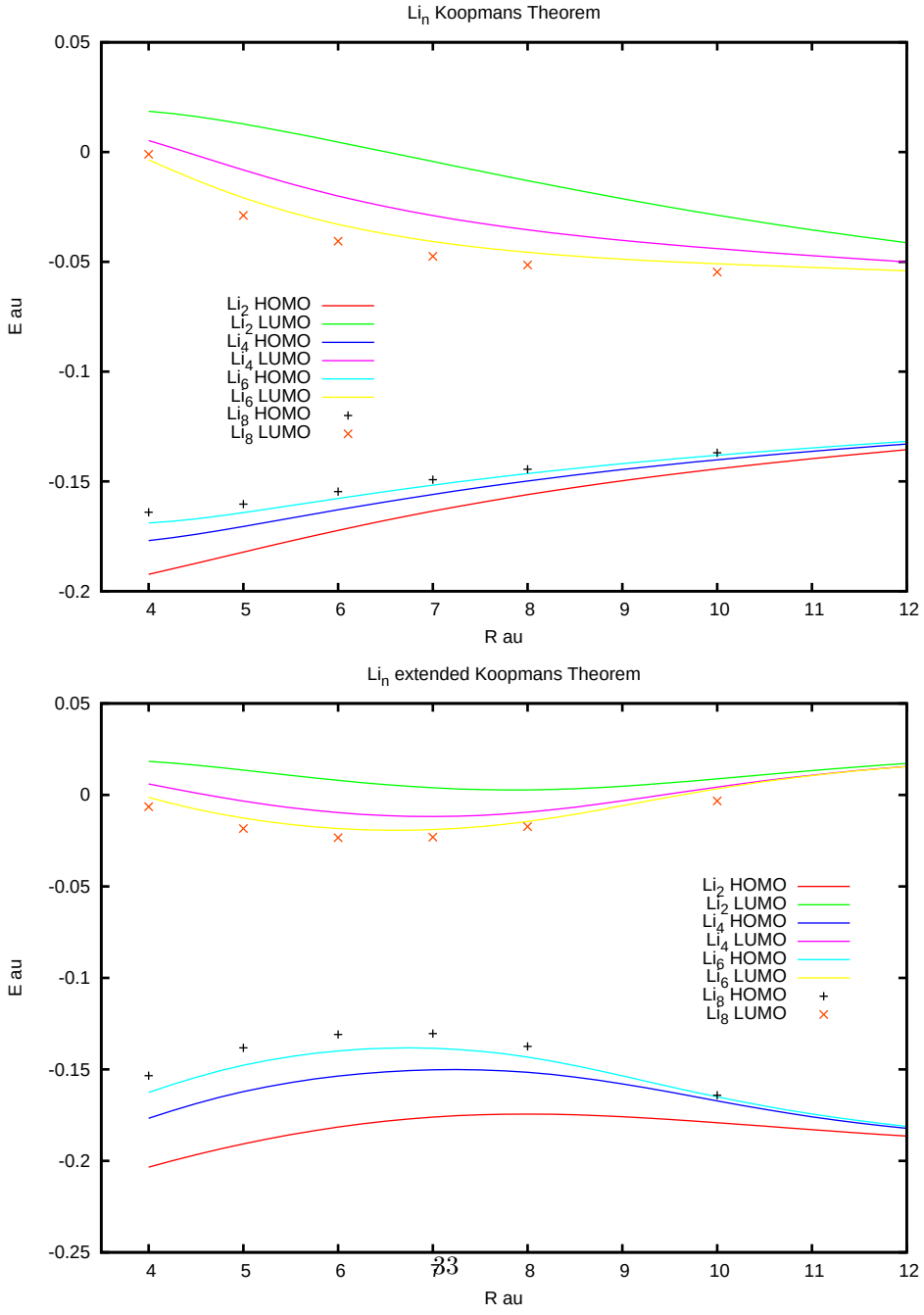

Figure 3: Koopmans' energy gaps as a function of the distance parameter R (bohr). Distances in bohr and energies in hartree.

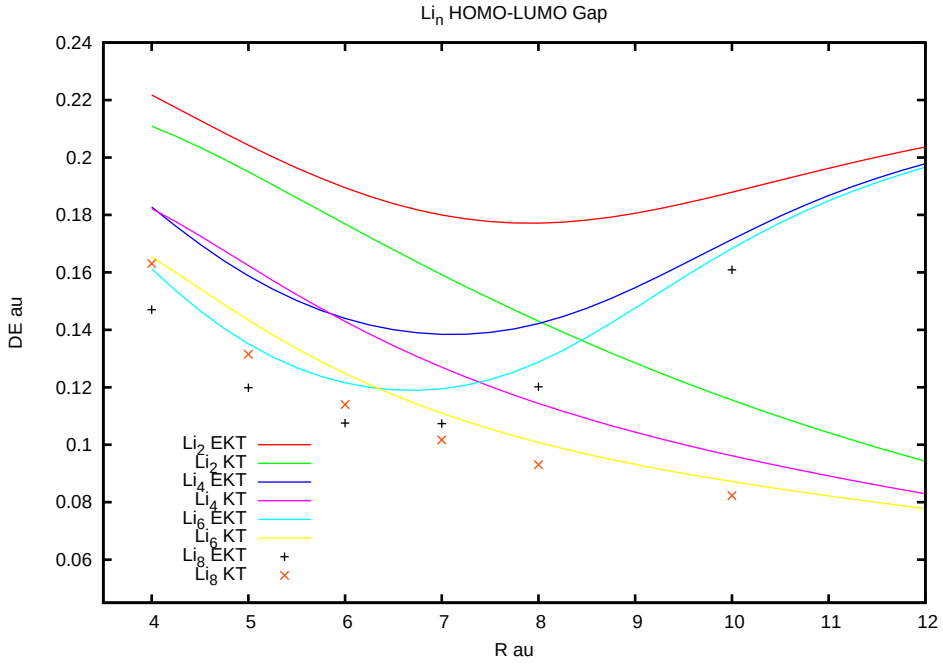

Figure 4: Exact energy gaps as a function of the distance parameter R (bohr). Distances in bohr and energy gaps in hartree.

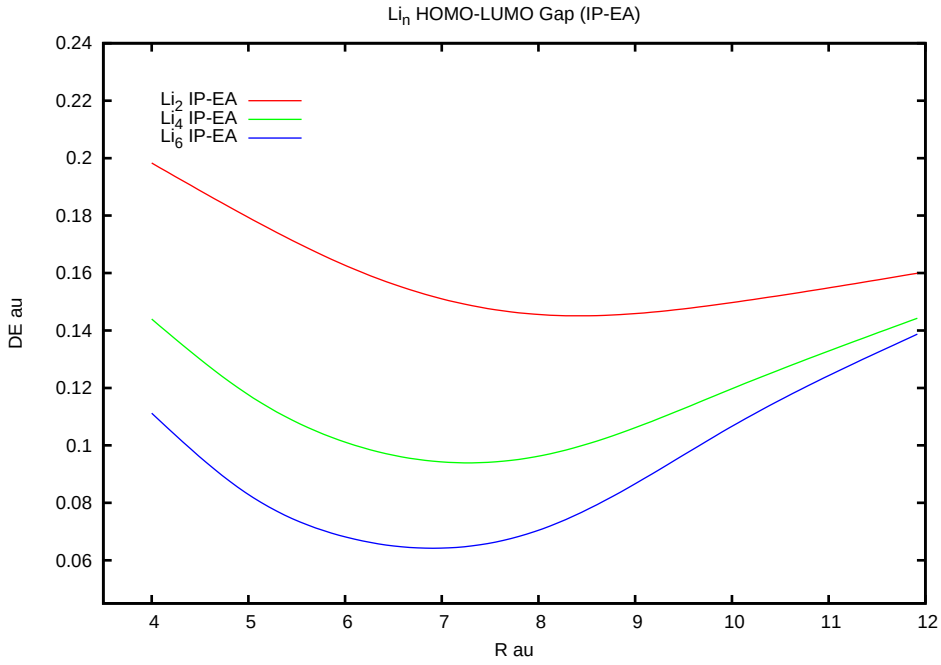

Figure 5: Specific (per atom) polarizabilities along the two main directions (orthogonal and parallel to the chain axes), as a function of the distance parameter R (bohr). **Figure 6a**: $\alpha_\perp$; **Figure 6b**: $\alpha_\parallel$ ($\alpha_\perp$ is also reported for comparison). Distance parameter R in bohr and polarizabilities α in 10^3 bohr^3.

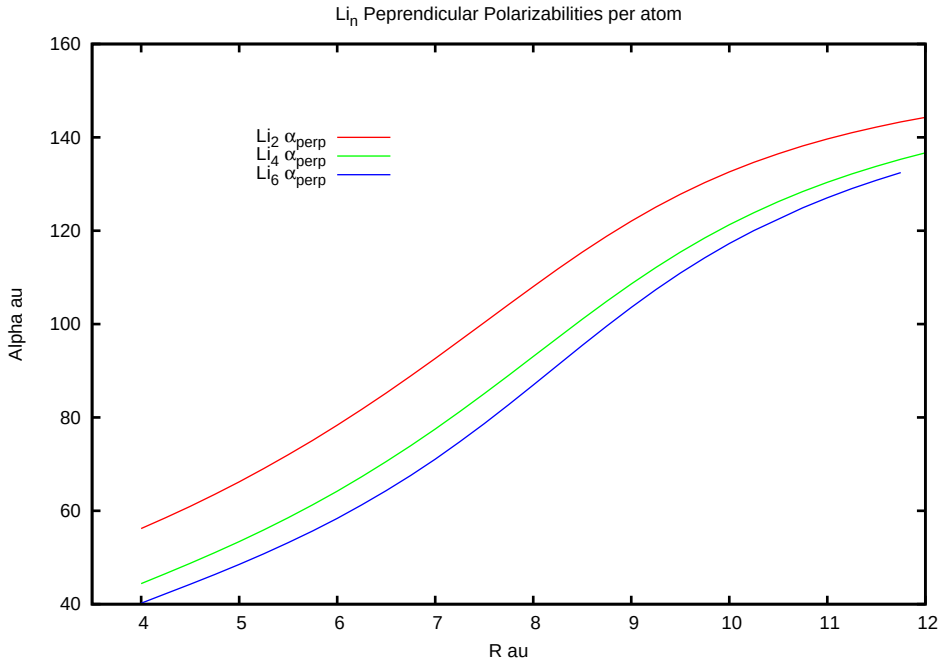

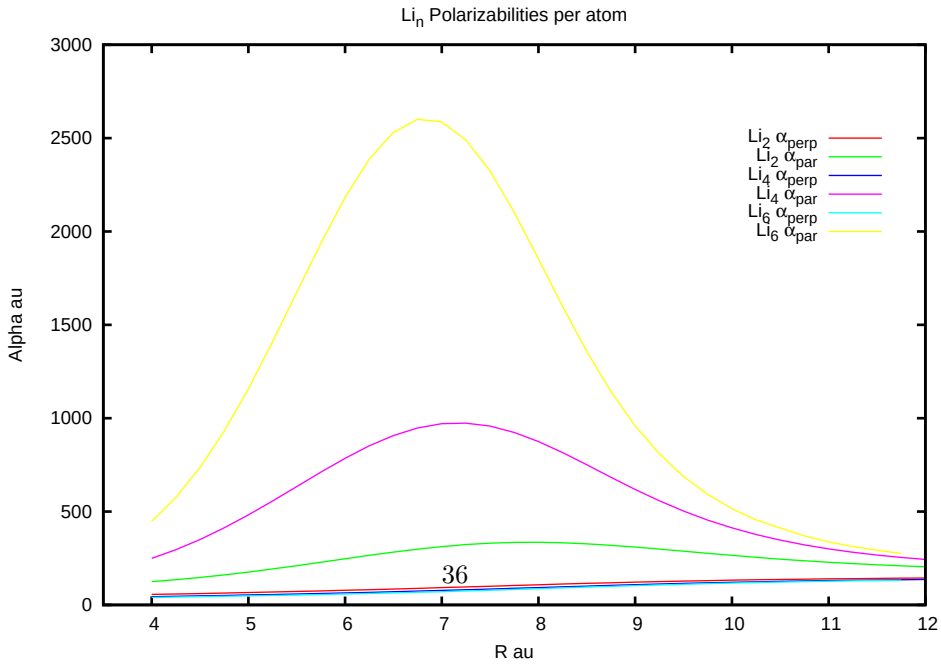

Figure 6: Localization tensor along the two main directions ($r_\perp$ and $r_\parallel$, orthogonal and parallel to the chain axes, respectively), as a function of the distance. Distance parameter R and localization tensor in bohr.